Applied Scientific Research **51**: 687–711, 1993.

Two dimensional linear stability of premixed laminar flames under zero gravity

H.S. MUKUNDA[1] & J.P. DRUMMOND[2]

[1]*Department of Aerospace Engineering, Indian Institute of Science, Bangalore 560 012, India*
[2]*NASA Langley Research Center, Hampton, Virginia, USA*

Received 6 September 1990; accepted in revised form 13 September 1992

Abstract. This paper reports on the numerical study of the linear stability of laminar premixed flames under zero gravity. The study specifically addresses the dependence of stability on finite rate chemistry with low activation energy and variable thermodynamic and transport properties. The calculations show that activation energy and details of chemistry play a minor role in altering the linear neutral stability results from asymptotic analysis. Variable specific heat makes a marginal change to the stability. Variable transport properties on the other hand tend to substantially enhance the stability from critical wave number of about 0.5 to 0.20. Also, it appears that the effects of variable properties tend to nullify the effects of non-unity Lewis number. When the Lewis number of a single species is different from unity, as will happen in a hydrogen-air premixed flame, the stability results remain close to that of unity Lewis number.

Nomenclature

A_f = Frequency factor for the forward reaction
A_b = Frequency factor for the backward reaction
Y_i = Mass fraction of species i
$\dot{\omega}_i'''$ = Volumetric reaction rate of species i
c_p = Specific heat at constant pressure
D_i = Trace diffusion coefficient ofspecies i
E = Activation energy
h_i = Enthalpy of species i
h_s = Sensible enthalpy of the mixture
h_{ct} = Heat of combustion of the reaction
h_i^o = Heat of formation of species i
$J_{i,j}$ = Jacobian of the reaction i with respect to species j
k = Wave number
Le_i = Lewis number of species i
M_i = Molecular weight of species i
ns = Number of Species = 4, here
p = Pressure
Pr = Prandtl number
R = Universal gas constant
Re = Reynolds number
s = Stoichiometric ratio
T = Temperature
T_r = Reference temperature = initial temperature
T_{ad} = Adiabatic flame temperature
t = Time
u = Streamwise velocity
v = Transverse velocity
x = Streamwise coordinate
y = Transverse coordinate
z = product of density and u velocity
κ = Conductivity
τ = Non-dimensional temperature
δ_f = Flame thickness
ϕ = Disturbance function
θ = Activation parameter
γ = Ratio of specific heats
ρ = Density
μ = Laminar viscosity
ω = Coefficient of time in the disturbance

Subscripts

f = Perturbed quantity
r = Value at reference condition
s = Steady state
i = Species identity, 1 for fuel, 2 for oxidizer, 3 for product and 4 for inert

Introduction

One dimensional laminar premixed flames can be obtained in the laboratory by premixing the gaseous fuel and oxidant in appropriate proportions and stabilising the flame in specially designed burners. Such flames are characterised by an upstream conduction-convection dominated region, a central reaction dominated zone and a downstream region containing product gases. The flames show a large decrease in density, and a very small change in pressure (because the dynamic pressure change is very small) through the flame. The stability of such flames has been a subject of study by a large number of workers. Starting with Landau [10] and Darrieus [4], a number of workers, including Margolis, Matkowsky, Sivashinsky and Clavin (see [2] for a detailed set of references) have contributed to this research. A scholarly review appears in Clavin [2]. Landau and Darrieus treated the one dimensional flame as a thin discontinuity across which density jump occurs. The dominant parameter that effects the stability is the disturbance wave length in a direction normal to the direction of propagation. They examined if such a lateral disturbance of wavelength, w (or wave number k) was amplified by the flow field. The leading order result is that the flame is unstable to all wave numbers. This result remained puzzling for a long time because stable laminar flames could be set up in laboratories. It is only later that effects of non-normal diffusion, curvature, and buoyancy on the flame stability were shown to reflect realistic features of stability. Studies by Sivashinsky, Matkowsky and others included the effects of non-normal diffusion (thermal and mass diffusion being unequal), first with low heat release and subsequently with significant heat release. The analysis of Pelce and Clavin [3], Matalon and Matkowsky [12], and Frankel and Sivashinsky [6] consider the limit of wave number tending to zero. The non-dimensionalization used are different in these analyses and the analysis of Pelce and Clavin is more general. One of the objectives of the three analyses conducted independently was to demonstrate the weak influence of viscosity in relation to conductivity and diffusivity. These studies obtain the dispersion relation (a result of the stability analysis giving the relationship between the growth rate and wave number) as $\omega = a(q)k - b(q, Le)k^2$ where ω is the growth factor, k the wave number, and a and b are coefficients depending on the temperature ratio ($T_{ad}/T_o = 1 + q$) and $Le = D\rho c_p/\kappa$, the ratio of mass to thermal diffusivities. The expressions for a and b obtained by Matalon and Matkowsky [12] as well as Frankel and Sivashinsky [6] do not match (after appropriate transformations) even for critical wave number. The numerical differences are not large in the interesting range of parameters and the values predicted for critical wave number are the same for $Le = 1$. Results based on systematic analysis and numerical integration of disturbance equations has been made by Jackson and Kapila [8]. Their numerical calculations have spanned the complete range of wave numbers and they confirm the earlier results in the appropriate limits. They deduce from such analysis the influence of exothermicity and buoyancy on flame stability [9]. Increase in exothermicity is shown to destabilise the flame and buoyancy stabilise the flame.

All these studies are analytical in nature and have treated the high activation energy limit. In these studies the steady state profiles for temperature, velocity and mass fractions are exponential in character and the reaction zone asymptotes to a plane. A typical plot from the calculations of Jackson and Kapila is shown in Fig. 1 for the largest parameter of exothermicity of [7] and without buoyancy. The parameter of exothermicity corresponds to a flame temperature six times the cold reactant temperature. The abcissa in Fig. 1 is $l = (1/Le - 1)E/RT_{ad}$. In this figure, m and θ are proportional to the activation energy, E for the finite rate chemistry models discussed later.

The results obtained are for $E/RT_{ad} \to \infty$ and for Lewis number not far from unity. It can be seen that at $l = 0$, corresponding to $Le = 1$, the unstable wave numbers are restricted to lower than 0.36. And as Le increases, the range of unstable wave numbers increases. Values of Lewis numbers of some species go up to 2 in the case of H_2-air systems. For $Le = 2.0$ and $E/RT_{ad} = 4$ for the H_2-air system, one obtains $l = -2$ and $k_{crit} = 0.6$. Thus the unstable wave number is increased substantially. At $Le = 1$, the unstable wave lengths are larger than 18 ($= 2\pi/k_{crit}$) times the flame thickness. The flame thickness is defined in these studies by $\delta_f = k_r/c_{pr}\rho_r u_r$ where k_r is the reference

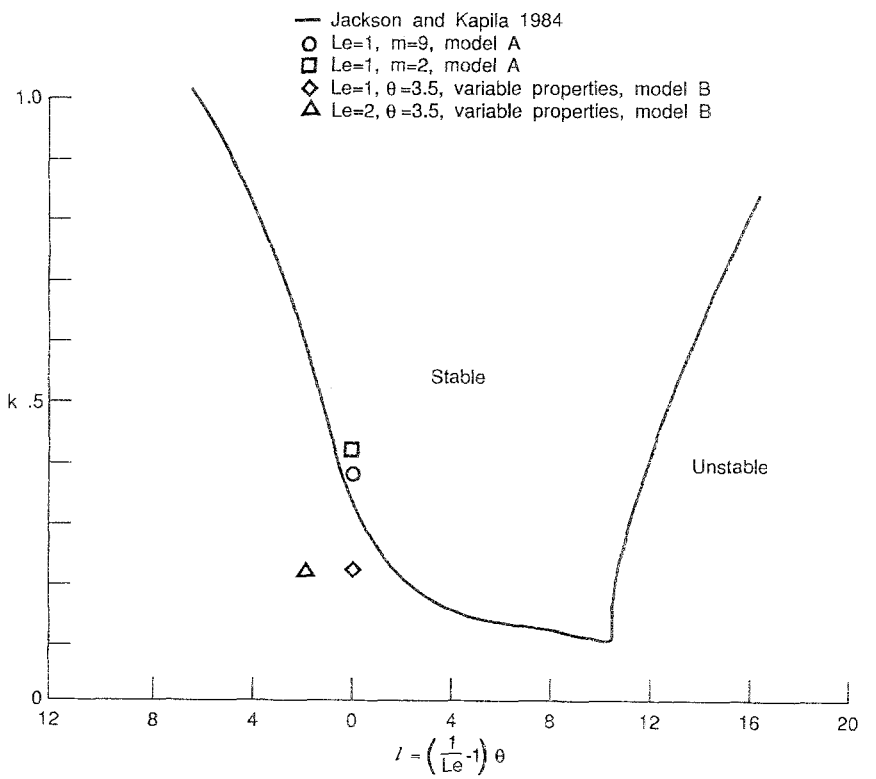

Fig. 1. Stability plot from calculations of Jackson and Kapila (1984) with some results from present calculations shown.

conductivity, c_{pr} is the specific heat, ρ_r = density and u_r, the flame speed. For cold reference conditions, this gives

$$\delta_f \simeq \frac{0.052\,\text{W/mK}}{(1390\,\text{J/kg K} \times 0.85\,\text{kg/m}^3 * 1.8\,\text{m/s})} \simeq 0.0000244\,\text{m}\ (0.0244\,\text{mm}).$$

For hot reference conditions, conductivity is almost 3.7 times the cold value and specific heat is 25% higher. The product of density and flame speed is constant for the respective cold and hot values, and $\delta_f \simeq 0.072$ mm. Therefore, the lateral wave length causing instability is $18\,\delta_f$, about 1.3 mm. In the above results, the principle controlling factor is hydrodynamics. The role of diffusion seems significant only for Lewis number departing from unity significantly.

As stated earlier, in all of the above analysis the activation energy is treated as large. The overall activation energy has been estimated by Fenn and Calcote [5] to be 16 kcal/g mole for H_2-air system and 28–30 kcal/g mole for many stoichiometric hydrocarbon air systems. At typical flame temperatures of 2300 K, the activation parameter $\theta = E/RT_{ad} \simeq 3.50$ for H_2-air and 6.1 to 6.5 for hydrocarbon-air mixtures. Arguments concerning the validity of asymptotic analysis are made after estimating θ to lie between 10 to 20 [2]. As noted above, the perceived values of overall activation energy for equivalent single step reaction are much smaller. While this departure may still permit the validity of asymptotic analysis, there needs to be demonstration of these aspects. Also, one may find that departures are small with regard to a few aspects, while for others, depending on the controlling phenomena, they are not.

Outline of the present work

Noting that the earlier work has examined the influences of gravity and thermal expansion on the stability, the present work considers the aspects like finiteness of the reaction and variable thermodynamic and transport properties on the stability of flames. The linear stability of flames is investigated numerically with particular reference to a stoichiometric H_2-air system by using a single step finite reaction model.

Two classes of reaction models termed Model A and Model B are treated. Both are finite distributed reaction models. Model A is chosen because of the possibility of obtaining exact analytical solutions to the steady state (or mean flow as is termed in stability analyses). It is primarily used to evaluate the effects of activation energy. Model B is in the line of classical single step reaction models where numerical solutions are needed even for steady state. In this model the effects of variable thermodynamic and transport properties as well as the effects of diffusion are explored in detail. In the single step reaction, there are four species, namely fuel ($i = 1$), oxidizer ($i = 2$), product ($i = 3$), and inert ($i = 4$). If we take that the diffusion is modelled after the trace diffusion approximation (see [10] for details) one has four Lewis numbers, Le_i, $i = 1$ to 4 defined by $Le_i = \rho D_i c_p/\kappa$, where D_i is the trace diffusion coefficient.

Instead of letting Le_i vary through the field something which is easily possible, different diffusion models are chosen to bring out explicitly the effects of diffusion. First of these takes all the Lewis numbers to be equal to unity. This forms the reference case explored by the other investigators in asymptotic analysis. The second model takes all the Lewis numbers to be equal to 2.0. This value is chosen to represent the Lewis number of the Hydrogen fuel in the environment of the other species. The third model takes $Le_1 = 2$ and $Le_j = 1, j = 2,3,4$. It is denoted by $Le = 2111$. This is chosen because in a typical Hydrogen-air flame the Lewis numbers for species other than Hydrogen are near unity. In addition, the sensitivity of the results to the accuracy of the steady state profiles is explored.

The analysis makes several assumptions and approximations some of which are discussed later. In particular, the variation of pressure and molecular weights in the equation of state are ignored.

The basic equations

The two-dimensional problem is set into an $x - y$ cartesian coordinate system, with the steady flame uniform in y and with variations along x. A simple step reaction, (fuel + oxidizer + inert) → (product + inert) is assumed. The conservation equations are nondimensionalised as follows:

$$\frac{x}{\delta_f} = \bar{x}, \frac{y}{\delta_f} = \bar{y}, \frac{tu_r}{\delta_f} = \bar{t}, \frac{\rho}{\rho_r} = \bar{\rho}, \frac{T}{T_r} = \bar{T}, \frac{u}{u_r} = \bar{u}, \frac{h_s}{c_{p,r}T_r} = \bar{h}_s, \tag{1}$$

$$\frac{v}{u_r} = \bar{v}, \frac{\kappa}{\kappa_r} = \bar{\kappa}, \frac{\mu}{\mu_r} = \bar{\mu}, \frac{D_i\rho}{(D\rho)_r} = \overline{D_i\rho}\,\frac{M_s}{M_r} = \bar{M}_s. \tag{2}$$

In the above equations h_s is the sensible enthalpy given by

$$h_s = \int_{T_r}^{T} \sum_{i=1}^{4} c_{p,i}\,\mathrm{d}T, \tag{3}$$

and M_s is the steady state average molecular weight of the mixture. The non-dimensionalized equations are put down by dropping bars.

$$\frac{\partial\rho}{\partial t} + \frac{\partial\rho u}{\partial x} + \frac{\partial\rho v}{\partial y} = 0, \tag{4}$$

$$\rho\frac{\partial u}{\partial t} + \rho u\frac{\partial u}{\partial x} + \rho v\frac{\partial u}{\partial y} = -\frac{\partial p}{\partial x} + \left(\frac{4}{3}\frac{\partial^2 u}{\partial x^2} + \frac{\partial^2 u}{\partial y^2} + \frac{1}{3}\frac{\partial^2 v}{\partial x\partial y}\right)\mathrm{Pr}, \tag{5}$$

$$\rho\frac{\partial v}{\partial t} + \rho u\frac{\partial v}{\partial x} + \rho v\frac{\partial v}{\partial y} = -\frac{\partial p}{\partial y} + \left(\frac{4}{3}\frac{\partial^2 v}{\partial x^2} + \frac{\partial^2 v}{\partial y^2} + \frac{1}{3}\frac{\partial^2 u}{\partial x\partial y}\right)\mathrm{Pr}, \tag{6}$$

$$\frac{\rho\partial h_s}{\partial t} + \rho u \frac{\partial h_s}{\partial x} + \rho v \frac{\partial h_s}{\partial y} = \frac{\partial}{\partial x}\left(\kappa \frac{\partial T}{\partial x}\right) + \frac{\partial}{\partial y}\left(\kappa \frac{\partial T}{\partial y}\right) - \sum_{i=1}^{ns} \frac{(h_i + h_i^o)}{c_{pr} T_r} \frac{\delta_f}{\rho_r u_r} \dot{\omega}_i''', \tag{7}$$

$$\frac{\rho\partial Y_i}{\partial t} + \rho u \frac{\partial Y_i}{\partial x} + \rho v \frac{\partial Y_i}{\partial y} = \frac{\partial}{\partial x}\left(D_i \rho \frac{\partial Y_i}{\partial x}\right) + \frac{\partial}{\partial y}\left(D_i \rho \frac{\partial Y_i}{\partial y}\right) + \frac{\delta_f}{\rho_r u_r} \dot{\omega}_i''', \quad i = 1, 2, 3, \tag{8}$$

$$\rho T = 1. \tag{9}$$

In the above equations $\dot{\omega}_i'''$ is the reaction rate of ith species. The primes denote the character of volumetric reaction rate. It is to be noted that for the single step reaction,

$$\dot{\omega}_1''' = \frac{\dot{\omega}_3'''}{s} = -\frac{\dot{\omega}_3'''}{(s+1)}, \tag{10}$$

where s = stoichiometric ratio, D_i are the diffusion coefficients chosen in the present study to give the Lewis number of the ith species a desired value. The mass fraction of the inert species ($i = 4$) is obtained from the identity that the four mass fractions must sum to unity.

The equation of state assumes pressure p is constant and is a good approximation for the stability study as well [12]. The variation in the molecular weight in the field is ignored (implying that M_s is unity). This is because the variation in the field is very small for most stoichiometric compositions, more particularly hydrogen-air mixture. This is due to the fact that the fraction of the fuel is to the extent of 2–4% in the mixture. This approximation is more true for fuel lean compositions. Even in fuel rich limit mixtures the importance of other quantities like conductivity and specific heat is so much more that one can ignore the variation of molecular weight. The momentum equations ignore the variation of viscosity in the field. This is assumed by noting the already demonstrated weak effects [2]. On the other hand, the variation of conductivity is accounted for because it is known to influence the stability characteristics significantly. The subscript r refers generally to cold upstream conditions, δ_f is the flame thickness chosen as $\delta_f = \kappa_r/(\rho_r u_r c_{pr})$. This implies that the Reynolds number based on the flame thickness is,

$$Re = \frac{\rho_r u_r \delta_f}{\mu_r} = \frac{\kappa_r}{\mu_r c_{pr}} = \frac{1}{\mathrm{Pr}}. \tag{11}$$

Thus the choice of δ_f as above implies that the product of Reynolds number and Prandtl number of the flame is unity. Another nondimensional number which appears in the equations is Schmidt number = Sc = $\bar{\mu}_r/(\overline{D\rho})_r$ which is set to unity to obtain $(\overline{D\rho})_r$.

These constitute the basic equations we need to solve.

The steady equations

Model A

As discussed earlier, the one-dimensional model utilises a formalism for which exact analytical solutions are available. The energy equation is set out as

$$\frac{d^2\tau}{d^2x} - \frac{d\tau}{dx} = -\frac{h_{ct}\delta_f \dot{\omega}'''}{\rho_r u_r (T_{ad} - 1)}, \tag{12}$$

where $\tau = (T - 1)/(T_{ad} - 1)$ and h_{ct} is the nondimensional heat of combustion.

The thermodynamic and transport properties are taken as constant and the relation reduces to $p =$ constant after ignoring viscous and inertial terms. The choice of the reaction term is discussed in the section on solutions.

Model B

This model utilises the same approximations as above, and the energy equation is set out similarly. The reaction equation and the rate expressions are,

$$2H_2 + O_2 \rightleftharpoons 2H_2O \tag{13}$$

$$\dot{\omega}''' = A_f p^3 Y_{H_2}^2 Y_{O_2} e^{-E_f/RT} - A_b p Y_{H_2O}^2 e^{-E_b/RT} \tag{14}$$

The choice of the forward rate constants is discussed later. The backward rate constants are chosen to be consistent with the equilibrium constant for the reaction noted above. The resulting one-dimensional equations are solved by a code specifically developed for the purpose [7].

The stability equations

For stability analysis, the independent variables chosen are $z = \rho u$, v, p, T and Y_i. The various quantities are expanded around steady state denoted by the subscript s, as

$$\begin{aligned}
\rho(x, y, t) &= \rho_s(x) + \rho_f(x)\phi(y, t) \\
z &= z_s(x) + z_f(x)\phi(y, t) \\
u &= u_s(x) + u_f(x)\phi(y, t) \\
v &= 0 + v_f(x)\phi(y, t) \\
p &= p_s(x) + p_f(x)\phi(y, t) \\
T &= T_s(x) + T_f(x)\phi(y, t) \\
Y_i &= Y_{s,i}(x) + Y_{f,i}(x)\phi(y, t)
\end{aligned} \tag{15}$$

$z_s(x) = \rho u_s(x) = 1$ because at steady state the equation of state gives constant mass flow through the flame. ϕ is chosen as

$$\phi = \exp(-j\omega t + jky), j = \sqrt{(-1)}. \tag{16}$$

Note that $j\omega = \omega_r + j\omega_i$ and the sign of ω_r decides the stability of the flame.

The stability equations for x-momentum contain u_f and u_f must be expressed in terms of other quantities. Manipulations of equation of state and the expression for z give

$$u_f = T_s z_f + T_f, u_s = T_s, \tag{17}$$

and

$$\rho_f = -T_f \frac{1}{T_s^2}. \tag{18}$$

The equations for model A

The following equations for z_f, p_f, v_f, and T_f, are obtained after the substitution of the expansions into the Eqs ((4)–(8)) and the subsidiary relations (17) and (18) are used.

$$z_f' + jk\frac{v_f}{T_s} = -i\omega\frac{T_f}{T_s^2}, \tag{19}$$

$$p_f' - T_s z_f'' + (T_s - 2T_s')z_f' + (k^2 T_s + T_s' - T_s'')z_f + J(T_s)T_f' = j\omega z_f, \tag{20}$$

$$v_f'' - v_f' - k^2 v_f - jkp_f = j\frac{\omega v_f}{u_s}, \tag{21}$$

$$T_f'' - T_f' + (J(T_s) - k^2)T_f - \frac{T_s'}{T_s}u_f = j\frac{\omega T_f}{T_s}, \tag{22}$$

where the primes denote the derivatives with respect to x. The term $J(T_s)$ is the Jacobian of the reaction rate and is obtained from steady state solutions to be discussed later (see Eq. 48). The above four set of equations constitute a seventh order system. These are solved under conditions of zero values as $x \to \pm\infty$ for all the variables, z_f, p_f, v_f and T_f. Since the number of boundary conditions is eight the problem is overdetermined and has nontrivial solutions for specific values of wave number, k. Thus the problem becomes one of eigen value.

The equations for model B

The following perturbation equations are obtained when Eqs (15) and (16) are used in Eqs (4–8) and the subsidiary relationships (17) are also used. The perturbation equations for z, v, p and T are

$$z'_f + jk\frac{v_f}{T_s} = -j\omega\frac{T_f}{T_s^2}, \tag{23}$$

$$p'_f - \mathrm{Pr}\left(\frac{4}{3}u''_f - k^2u_f + j\frac{k}{3}v'_f\right) + u'_s z_f + u'_f = j\omega\frac{u_f}{T_s}, \tag{24}$$

$$v''_f - \frac{3}{4\mathrm{Pr}}v'_f - \frac{3}{4}k^2v_f + jk\frac{u_s}{4}z'_f + jk\frac{u'_s}{4}z_f + j\frac{k}{4}T'_f - j\frac{3}{4\mathrm{Pr}}kp_f = j\omega v_f\frac{3}{4\mathrm{Pr}}\frac{1}{T_s}, \tag{25}$$

$$T''_f + \left(\frac{-\bar{c}_p}{\kappa_s} + \frac{2}{\kappa_s}\frac{d\kappa_s}{dT}T'_s\right)T'_f - \left(k^2 + \frac{1}{\kappa_s}\sum_{i=1}^{ns}\frac{(h_i + h_i^o)}{c_{pr}T_r}\frac{\delta_f}{\rho_r u_r}J_{i,T}\right)T_f$$
$$- \frac{1}{k_s}\sum_{i=1}^{ns}\frac{(h_i + h_i^o)}{c_{pr}T_r}\sum_{j=1}^{ns}\frac{\delta_f}{\rho_r u_r}J_{i,j}Y_{j,f} - \frac{\bar{c}_p}{\kappa_s}T'_s z_f = -j\frac{1}{T_s}\frac{\bar{c}_p}{\kappa_s}\omega T_f, \tag{26}$$

$$Y''_{i,f} - k^2Y_{i,f} + \left(-\frac{1}{(D_i\rho)_s} + \frac{1}{(D_i\rho)_s}\frac{d(D_i\rho)}{dT_s}T'_s\right)Y'_{i,f}$$
$$+ \frac{1}{(D_i\rho)_s}\frac{\delta_f}{\rho_r u_r}\left[J_{i,T}T_f + \sum_{j=1}^{ns}J_{i,j}Y_{j,f}\right]$$
$$- \frac{1}{D_i\rho_s}Y'_{i,s}z_f\frac{1}{(D_i\rho)_s}\frac{d(D_i\rho)}{dT_s}Y'_{1,s}T'_f = -j\frac{1}{T_s}\frac{1}{(D_i\rho)_s}\omega Y_{i,f}, \tag{27}$$

where

$$\bar{c}_p = c_{p,s} + T_s\frac{dc_p}{dT_s}, \tag{28}$$

$$J_{i,j} = \frac{\partial\dot{\omega}_i'''}{\partial Y_j},\quad J_{i,T} = \frac{\partial\dot{\omega}_i'''}{\partial T}. \tag{29}$$

It is possible to relate the Jacobians $J_{i,j}$ and $J_{i,T}$ amongst themselves by invoking the stoichiometric relations between the reaction rates (Eq. 8) to obtain

$$sJ_{1,j} = J_{2,j},\ -(s+1)J_{1,j} = J_{3,j},\ sJ_{1,T} = J_{2,T},\ -(s+1)J_{1,T} = J_{3,T} \tag{30}$$

In treating the variation of properties it is assumed that all the dependence of the thermodynamic and transport properties in the flow field is described in terms of temperature alone. This is not entirely correct since there is some dependence on mass fractions of various species as well. But for premixed mixtures, it is reasonably accurate, certainly at Lewis number of unity where all the properties are described in terms of one progress variable namely temperature. For nonunity Lewis numbers, the approximation implies that the extra dependence on mass fractions is ignored. The equation for pressure is in terms of u_f and its derivatives. They can be expressed in terms of z_f and T_f using relations in (17) to obtain an equation for p_f given by,

$$p_f' - \frac{\mathrm{Pr}}{3}(4u_s'' z_f + 8u_s' z_f' + 4u_s z_f'' + 4T_f'' - 3k^2 u_s z_f - 3k^2 T_f + jkv_f') + 2u_s' z_f + u_s z_f' + T_f' = j\omega z_f + j\omega \frac{T_f}{T_s}. \tag{31}$$

The primes on various quantities represent derivatives with respect to x. As can be noted, the perturbation equations require u_s, derivatives of u_s (up to the second order), first derivatives of T_s and Y_i, and Jacobians of reaction rate with respect to T and Y_i.

There is a further possibility of reducing the order of equations. One should normally solve three species conservation equations. However, the perturbation on the summation of mass fractions leads to

$$Y_{1,f} + Y_{2,f} + Y_{3,f} = 0. \tag{32}$$

Hence it is sufficient to solve only two of the species conservation equations. The energy and species equations must be recast using the relations given in (8). For this case, we get

$$T_f'' + \left(\frac{-\bar{c}_p}{\kappa_s} + \frac{2}{\kappa_s}\frac{d\kappa_s}{dT}T_s'\right)T_f' - \left(k^2 + \frac{1}{\kappa_s}h_{ct}\frac{\delta_f}{\rho_r u_r}J_{1,T}\right)T_f - \frac{1}{\kappa_s}h_{ct}\frac{\delta_f}{\rho_r u_r}[(J_{1,1}-J_{1,3})Y_{1,f} + (J_{1,2}-J_{1,3})Y_{2,f}] - \frac{\bar{c}_p}{\kappa_s}T_s' z_f = -j\frac{1}{T_s}\frac{\bar{c}_p}{\kappa_s}\omega T_f, \tag{33}$$

$$Y_{1,f}'' + \left[-k^2 + \frac{1}{(D_1\rho)_s}\frac{\delta_f}{\rho_r u_r}(J_{1,1}-J_{1,3})\right]Y_{1,f} - \frac{1}{(D_1\rho)_s}\frac{\delta_f}{\rho_r u_r}(J_{1,2}-J_{1,3})Y_{2,f} - \frac{1}{(D_1\rho)_s}Y_{1,f}' - \frac{1}{D_1\rho_s}Y_{1,s}' z_f + \frac{1}{(D_1\rho)_s}\frac{\delta_f}{\rho_r u_r}J_{1,T}T_f + \frac{1}{(D_1\rho)_s}\frac{d(D_1\rho)}{dT_s}T_s' Y_{1,f}' + \frac{1}{D_1\rho_s}\frac{d(D_1\rho)}{dT_s}Y_{1,s}' T_f' = -j\frac{1}{T_s}\frac{1}{(D_1\rho)_s}\omega Y_{1,f}, \tag{34}$$

$$Y''_{2,f} + \left[-k^2 + \frac{1}{(D_1\rho)_s} \frac{\delta_f}{\rho_r u_r} (J_{2,1} - J_{2,3}) \right] Y_{2,f} - \frac{1}{(D_2\rho)_s} \frac{\delta_f}{\rho_r u_r} (J_{2,1} - J_{2,3}) Y_{1,f}$$
$$- \frac{1}{(D_2\rho)_s} Y'_{2,f} - \frac{1}{(D_2\rho)_s} Y'_{2,s} z_f + \frac{1}{((D_2\rho))_s} \frac{\delta_f}{\rho_r u_r} J_{1,T} T_f$$
$$+ \frac{1}{(D_2\rho)_s} \frac{d(D_2\rho)}{dT_s} T'_s Y'_{1,f} + \frac{1}{D_2\rho_s} \frac{d(D_2\rho)}{dT_s} Y'_{2,s} T'_f = -j \frac{1}{T_s} \frac{1}{(D_2\rho)_s} \omega Y_{2,f}. \tag{35}$$

In obtaining the above equations, the following equalities obtained from Eq. (30) have been used.

$$J_{2,2} - J_{2,3} = s(J_{1,2} - J_{1,3}),\ J_{2,1} - J_{2,3} = s(J_{1,1} - J_{1,3}), \tag{36}$$

$$h_{ct} = [h_1 + h_1^o + s(h_2 + h_2^o) - (1 + s)(h_3 + h_3^o)]/(c_{pr} T_r). \tag{37}$$

If the choice of Lewis numbers is such that $Le_2 = Le_3$, then the two species equations can be related by $sY_{2,f} = -(s + 1)Y_{3,f}$. This equation can be used to reduce the number of species equations to 1 and to modify the energy equation. Such a modification gives

$$T''_f + \left(\frac{-\bar{c}_p}{\kappa_s} + 2k_s \frac{d\kappa_s}{dT_s} T'_s \right) T'_f + \left(-k^2 + \frac{1}{\kappa_s} h_{ct} \frac{\delta_f}{\rho_r u_r} J_{1,T} \right) T_f$$
$$- \frac{1}{\kappa_s} h_{ct} \frac{\delta_f}{\rho_r u_r} J_\sigma Y_{1,f} - \frac{\bar{c}_p}{\kappa_s} T'_s z_f = -j \frac{1}{T_s} \frac{\bar{c}_p}{\kappa_s} \omega T_f, \tag{38}$$

$$Y''_{1,f} + \left[-k^2 + \frac{1}{D_1\rho_s} \frac{\delta_f}{\rho_r u_r} J_\sigma \right] Y_{1,f} + \left(\frac{-1}{(D_1\rho)_s} + \frac{1}{(D_1\rho)_s} \frac{dD_1\rho}{dT_s} \right) T'_s Y'_{1,f} - \frac{1}{(D_1\rho)_s} Y'_{1,s} z_f$$
$$+ \frac{1}{(D_1\rho)_s} \frac{\delta_f}{\rho_r u_r} J_{1,T} T_f + \frac{1}{(D_1\rho)_s} \frac{dD_1\rho}{dT_s} Y'_{1,s} T'_f = -j\omega \frac{1}{T_s} \frac{1}{(D_1\rho)_s} Y_{1,f},$$

where

$$J_\sigma = J_{1,1} + sJ_{1,2} - (1 + s)J_{1,3}. \tag{40}$$

In this case the order of the equation to be solved is 9. If $Le_i = 1$, one can eliminate the equation for Y_1 by combining with energy equation. The perturbation equation for enthalpy will have zero for the solution. For this case, $(D_1\rho)_s = (\kappa_s/\bar{c}_p)$ and the temperature gradient terms associated with the transport properties are ignored. In this case the energy equation becomes

$$T''_f - \frac{\bar{c}_p}{\kappa_s} T'_f - T_f \left[k^2 + \frac{1}{\kappa_s} \frac{\delta_f}{\rho_r u_r} (J_\sigma - h_{ct} J_{1,T}) \right] - \frac{\bar{c}_p}{\kappa_s} \frac{dT_s}{dx} z_f = -j \frac{1}{T_s} \frac{\bar{c}_p}{\kappa_s} \omega T_f. \tag{41}$$

The steady state solutions—model A

Recognising the fact that the Eq. (12) does not have the space co-ordinate explicitly, it is possible to reduce the order of the equation by defining $q = (d\tau/dx)$ (Spalding, [5]). One can then recast the equation as

$$q\left(\frac{dq}{d\tau} - 1\right) = -\Lambda\dot{\omega}''', \tag{42}$$

where Λ represents the constants on the right hand side of Eq. (42). Equation (42) has been subjected to analysis in combustion literature. The reaction rate expression starts from exponentially small values near $\tau = 0$ peaks at some value of τ depending on the activation energy and goes to 0 at $\tau = 1$. Similarly q is 0 both at $\tau = 0$ and 1 and is positive definite over the range $\tau = 0$ to 1 for the adiabatic case considered here. Based on these observations one can show that for a class of profiles $q = \tau - \tau^m$ where m is a parameter, one obtains $\Lambda = 1$ and $\dot{\omega}''' = m\tau^m(1 - \tau^{(m-1)})$. Reversing the above argument, one can say that for the reaction rate expression just indicated (with m as a parameter), the solution for q is as stated earlier. One can integrate the equation for q and set out the steady state solution as

$$\tau_s = [1 + \exp(-(m-1)x + c)]^{-1/(m-1)}, \tag{43}$$

$$T_s = \tau_s(T_{ad} - 1) + 1, \tag{44}$$

$$u_s = T_s, \tag{45}$$

$$\frac{dT_s}{dx} = (T_{ad} - 1)\frac{d\tau_s}{dx} = (T_{ad} - 1)(\tau_s - \tau_s^m), \tag{46}$$

$$\dot{\omega}''' = m\tau_s^m(1 - \tau_s^{(m-1)}), \tag{47}$$

$$J = \frac{\partial\dot{\omega}'''}{\partial T} = (T_{ad} - 1)m^2\tau_s^{(m-1)}\left[1 - \left(2 - \frac{1}{m}\right)\tau^{(m-1)}\right]. \tag{48}$$

In the above equations, the steady state result that $(\rho u)_s = 1$ along with the equation of state is used to obtain equation (45). c in Eq. (44) is chosen so as to fix $\tau = 0.5$ at $x = 0$. This gives

$$c = \log(2^{(m-1)} - 1) \tag{49}$$

The solutions noted above are coded and used in the solution of the stability equations. It must be noted that the choice of c has no effect excepting on the resolution of the eigen-solutions. With the stability code using a grid distribution which allows finer resolution at the centre ($x = 0$) and increasingly coarse grid at x far removed from this point, one expects better resolution by arranging the steady solution in this manner. The stability code utilises its own grid distribution and

computes the various quantities using the analytical expressions noted above. The parameter m characterises essentially the activation energy i.e. m = constant (E/RT_{ad}). Typically values of $m \doteq 4 - 6$ imply high activation energy and $m \doteq 1.3$ implies activation energies close to 16 kcal/mole of a range expected for H_2-air system. This fact is based on the result that the reaction rate distribution, Eq. (47) has peak at τ_s close to 0.5, a feature seen later even with reaction rate distribution with τ in the case of full chemistry.

The steady state solutions—model B

The numerical solutions for the assumed reaction rate for the H_2-air system are obtained from an unsteady code developed for the purpose [7]. The code also generates the Jacobians of reaction rate with respect to temperature and mass fractions of species to be used in the stability code. These steady state results are used in the stability calculations for non-unity Lewis number cases. The steady problem uses a uniform grid in $z = \int \rho \, dx$. The grid is then transformed to the $x = \int dz/\rho$ coordinate. Then, the results of temperature, mass fractions, Jacobians are interpolated using a cubic spline interpolation program into the grid required by the stability code. The temperature data then are spectrally differentiated by a Chebychev polynomial fit to obtain the first and the second derivatives. These profiles were found to be jagged and nonsmooth. Consequently, it was decided to curve fit those data which needed to be differentiated. A Pade polymonial fit was used to describe the temperature distribution with x and molecular weight, specific heat, conductivities and diffusivities with temperature. These were then used in the stability code.

The stability solutions-numerical aspects

The stability code used here was originally written for analysing the stability of high speed flows [11]. The perturbation equations are discretized by a spectral collocation technique using Chebychev polynomials as basis functions. The code utilizes a staggered mesh to treat pressure. The resulting discretized equations are set out into a generalized matrix eigenvalue problem and are solved using the standard library routine [11].

Model A

In this case, all the steady state quantities were known in analytical form and the calculations on the stability could be performed in a straightforward manner. The code utilized a grid stretching with finest portion of the grids at $x = 0$. The region covered is from $-\infty$ to ∞. It was therefore necessary to set a value for infinity. Several initial experiments suggested that the infinity could be set at $x = \pm 15$. In a few cases,

the eigenfunction could not be resolved accurately since the decay was slow and for this purpose an infinity range was extended to ± 20. (It must be remembered that this x is already nondimensionalized by δ_f). Grid resolution studies were conducted and these showed that the results did not differ by more than 0.1% when this number of grid points exceeded 121. Most calculations reported here utilized at least 121 grid points. An interesting aspect of the eigenfunction distribution concerned the fact that in most cases, pressure perturbations decayed the slowest towards the boundaries. Initial concerns regarding the effect on accuracy was resolved when it was determined that enhancing the boundaries and increasing the grid resolution did not affect the critical neutral wave number, but altered the eigenfunctions marginally.

Model B

Regarding the questions of the range of infinity and grid resolution, the experiences noted earlier are found to be valid. It should be noted that in the numerical results of steady flames, it was necessary to define a value of δ_f. While it would be possible to estimate it from $\delta_f = k_r/\rho_r u_r c_p r$, it was convenient to assign a value δ_f, and from this, obtain a consistent set of reference values. It should be remembered that the critical wave number, a result from the stability code is actually a non-dimensional quantity, the non-dimensionalising parameter being δ_f. One would expect that the physical results obtained are independent of the choice of δ_f. This was ensured by varying the value of δ_f and obtaining the critical wavelength independent of δ_f in one case.

Results and discussion

a. Model A

Figure 2 shows the steady state profile of temperature, its first gradient the second gradient and the Jacobian. Most of the region of large change is restricted to a region $-4 \leqslant x \leqslant 4$. The Jacobian varies significantly over the field and the variation is different for $m = 9$ and 2. The variation is larger for larger m and smaller for smaller m. The calculations lead to a set of critical wave numbers (zero growth rate $\omega_i = 0$) versus m, the activation energy parameter, as shown in Table 1. The peaks of the eigenfunctions are shown in the table for the cases U and P, the unperturbed and the perturbed to be discussed below. It can be seen from the table that the critical wave number varies from 0.36 at high m to about 0.40 at $m \simeq 1.3$ corresponding to $E \simeq 68.9$ kJ/mole. This constitutes a 10% change and is not considered significant. The eigenfunctions are consistent with results from the asymptotic analysis. The imaginary part of z_f, real part of v_f, imaginary parts of T_f and p_f are zero. The other non-zero eigenfunctions are normalized by the peak of p_f.

In studies of stability with strong convection such as mixing or boundary layers, it is found that the mean profile exerts a significant influence on the stability character-

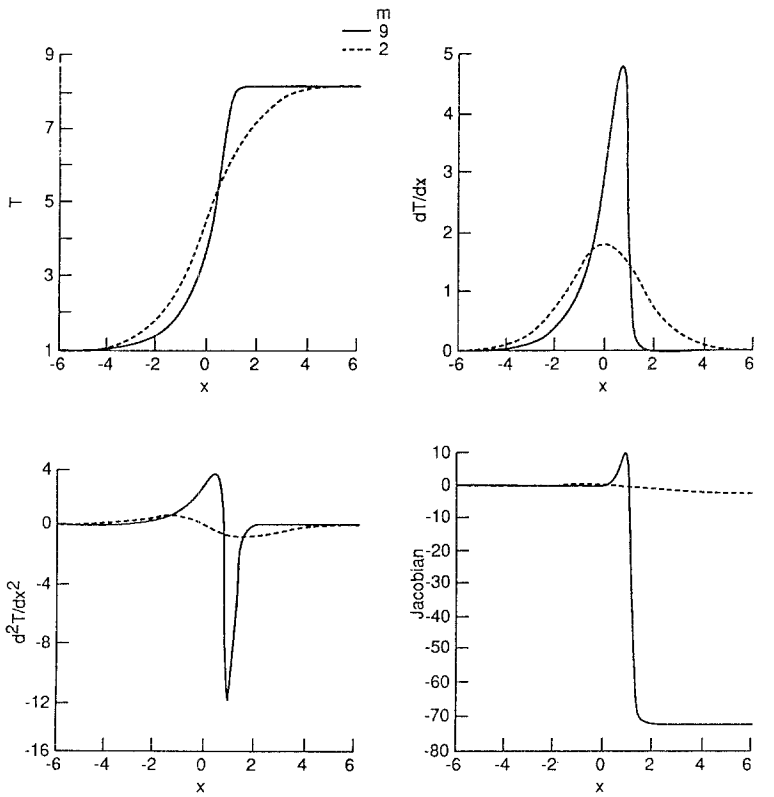

Fig. 2. Steady-state profiles of temperature, first gradient, second gradient, and Jacobians for $m=9$ and 2.

Table 1. Case: Model A

a. Critical wave number k_{crit} versus m

m	*Unperturbed case, k_{crit}*	*Perturbed case, k_{crit}*
9	0.362	0.3704
4	0.375	0.382
2	0.391	0.407
1.3	0.401	0.411

b. Peaks of eigen functions

m	Rl *z*	Im *v*	Rl *T*	Rl *p*
9 *U*	2.9	17.5	74.0	210.0
9 *P*	3.3	19.2	79.1	225.6
2 *U*	8.2	28.1	78.3	58.3
2 *P*	9.1	29.3	79.7	62.5

U = Unperturbed, *P* = Perturbed

istics. In order to determine the validity of this statement in the present context, and in addition to determine the features which affect stability significantly, subsidiary calculations were performed as follows. The initial profile of $T_s'(x)$ and $T_s''(x)$ were perturbed by a function

$$4x(\dot{x}_\infty - x)/x_\infty^2 \sin\frac{3\pi}{2}\frac{x}{x_\infty}$$

chosen arbitrarily so that there would be fluctuations in the profile with zero at the boundaries $x = 0$ and $x = x_\infty$. Figure 3 shows the plots of steady profiles. As can be seen, both dT/dx and d^2T/dx^2 profiles have considerable fluctuations. Table 1 shows the comparison of k_{crit} and peak amplitudes of eigenfunctions for $m = 9$ and $m = 2$. The k_{crit} is altered by no more than 3% and the eigenfunctions, are altered somewhat more, but less than 10%. There are considerable fluctuations in the resulting eigenfunctions, largely those for pressure. These fluctuations do not seem to affect the overall result on stability. Thus the errors in temperature profile gradients seem to make little difference to the results of stability. The reason for this is that the instability is largely driven by hydrodynamics and details of the profile do not matter

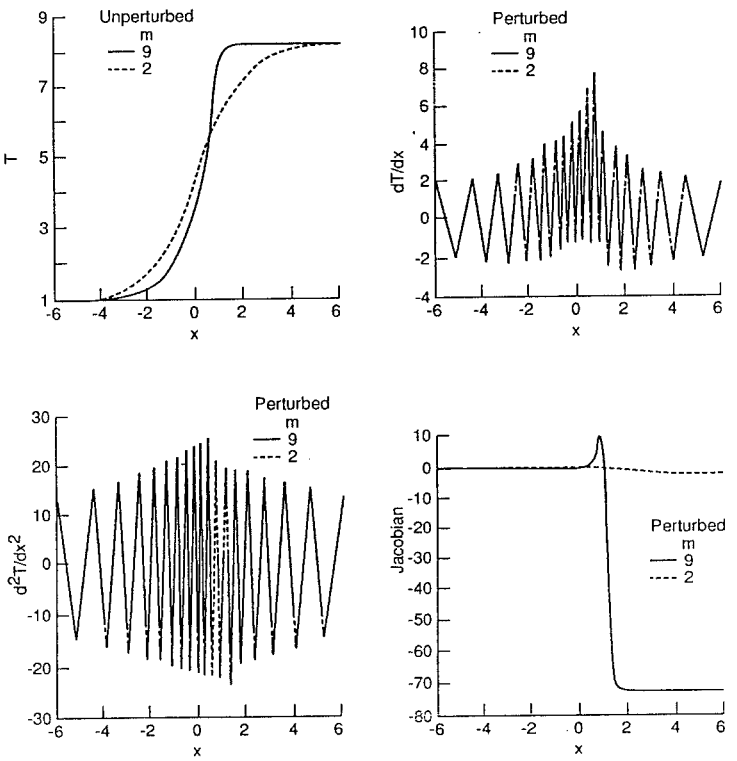

Fig. 3. Steady profiles with and without perturbations for $m=9$ and 2.

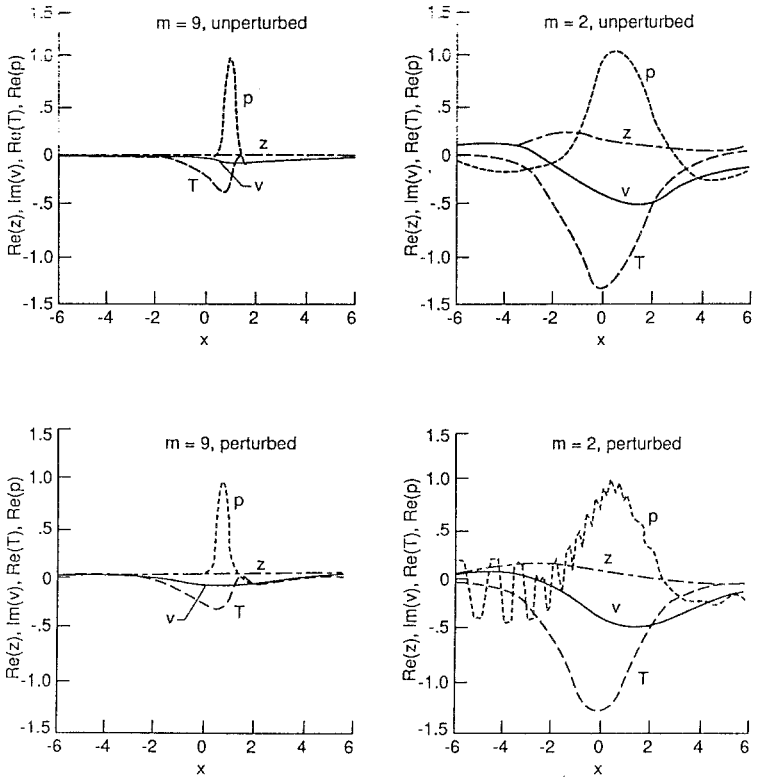

Fig. 4. Eigenfunctions for $m=9$ and 2, unperturbed and perturbed.

significantly. Figure 4 shows the eigenfunctions for both low and high activation energies, between the cases where the profiles are perturbed and the reference or unperturbed. Firstly consider the case with no perturbations (U). The structure of the eigenfunctions shows that their width is also about ± 4. It is only the eigenfunction for pressure that seems to decay slowly. For the case of reduced activation energy, the temperature eigenfunction peak is larger than the pressure eigenfunction. This feature of the temperature eigenfunction having a peak higher than the pressure eigenfunction is seen in all the later calculations using the chemistry model B. Between these two cases U and P the effect of disturbance is less severe for $m = 9$ than for $m = 2$. Calculations were made by changing the Jacobian by 5% from the nominal value. This results in a substantial change in the critical wave number of 20%. The features concerning the eigenfunctions look very similar and seem altered quantitatively to a small extent. Thus the stability is very sensitive to the Jacobians but quite insensitive to the details of temperature profile gradients.

The effect of Prandtl number has been discussed by earlier workers [2] and were deduced to be insignificant. The results of the dependence of the critical wave number on Prandtl number are presented in Table 2. The changes of k_{crit} near Pr = 1 are marginal. Only in the extreme case of Pr = 0.05 does the change of k_{crit} from that of

Table 2. Case: Model B

a. Critical wave number k_{crit} versus Prandtl number

Pr	k ($m = 9$)	k ($m = 2$)
1.0	0.391	0.362
0.7	0.377	0.374
0.1	0.305	0.331
0.05	0.300	0.301

Pr = 1 look substantial. A study that considered Pr → 0 was conducted to determine if the viscous terms could be neglected altogether. Two calculations were made by dropping the viscous terms in the u and v momentum equations separately. Neglecting the viscous terms in the u equation for the case $m = 2$ leads to a 10% reduction of k_{crit} from 0.391 to 0.356. Neglecting viscous terms in the v equation does not lead to an acceptable solution satisfying the boundary conditions. This situation is inferred to be related to the neglect of the highest order derivatives in v (v'' term) which is a typical singular perturbation problem. This is why the approach of obtaining the limiting solution by letting Pr → 0 by retaining all the derivatives seems to lead to a physically consistent result.

a. Model B

Numerical calculations for a steady flame were performed for the stoichiometric H_2-air system with a single step reaction scheme, $2H_2 + O_2 \rightleftharpoons H_2O$, with frequency factor = $A_f = 1.1 \times 10^{19}$, and an activation energy, $E = 16$ kcal/mole. The choice of the parameters was based on the calculations of the stoichiometric flame structure with full chemistry [1]. Figure 5 shows the plot of reaction rate of hydrogen with nondimensional temperature from such a calculation. The peak in the reaction rate occurs at $T \simeq 4.2$ whereas the adiabatic temperature corresponds to $T = 8.156$. For $Le = 1$, the reaction rate expression becomes a function depending on temperature alone. Now, one can estimate E (or θ) from the plot of reaction rate with temperature. Such a calculation yields $E \simeq 16$ kcal/mole. Such estimates are also available from earlier work (Fenn and Calcote, [5]).

The steady flame speeds obtained from the steady state calculations are 1.63 ($Le = 1$), 1.83 ($Le_i = 2$), 1.70 m/s ($Le_i = 2111$). The case $Le_i = 2111$ implies that the Lewis numbers for the four species 1,2,3,4 are 2,1,1 and 1. The results of the steady profiles and the eigenfunctions for the nominal case are shown in Fig. 6. The critical wave number for chosen values of δ_f are shown in Table 3. As can be seen, the critical unstable wavelength is about 0.9 mm for the classical constant property case. For large activation energy, the critical wavelength would be about 1.05 mm (not shown in the tables).

The calculations with variable properties show results which are interesting. Variable properties seem to act as a stabilising influence, raising the unstable

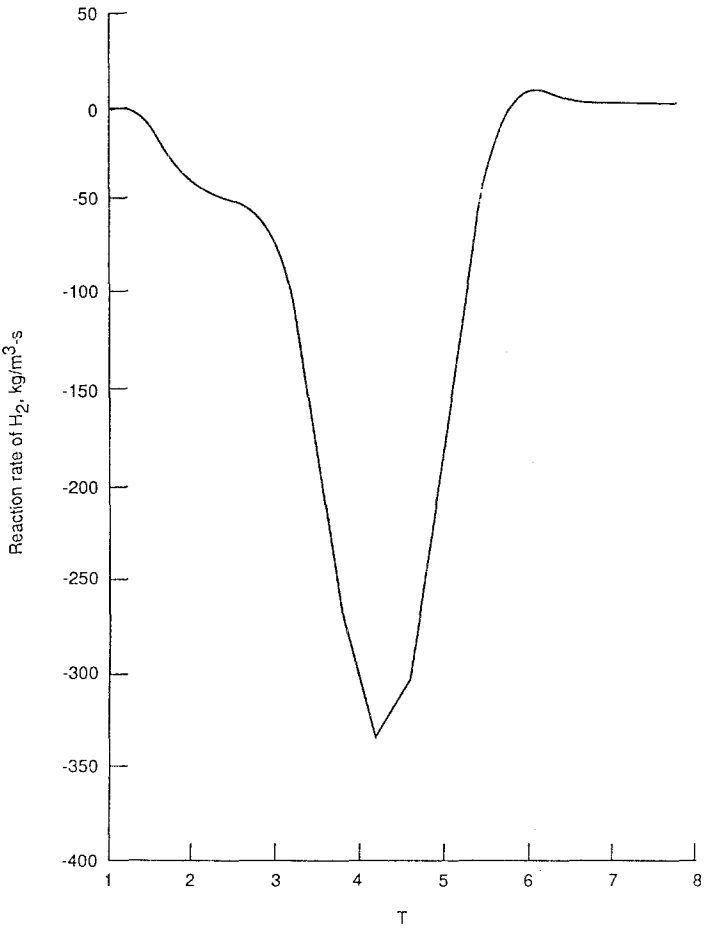

Fig. 5. Reaction rate of H_2 with temperature for full chemistry.

Table 3. Case: Model B, $Le = 1$, $\theta = 3.5$

a. Critical wave number k_{crit} and δ_f

Case	k_{crit}	δ_f mm	*Wavelength*, mm $=2\pi\delta_f/k_{crit}$
Const. prop	0.42	0.06	0.9
Var. prop	0.20	0.06	1.88
Var. c_p	0.43	0.06	0.88
Var. κ and $D\rho$	0.18	0.06	2.09

b. Peaks of eigen functions

Case	Rl z	Im v	Rl T	Rl p
Const. prop	10.0	26.0	83.8	64.5
Var. prop	8.0	25.0	74.4	66.5

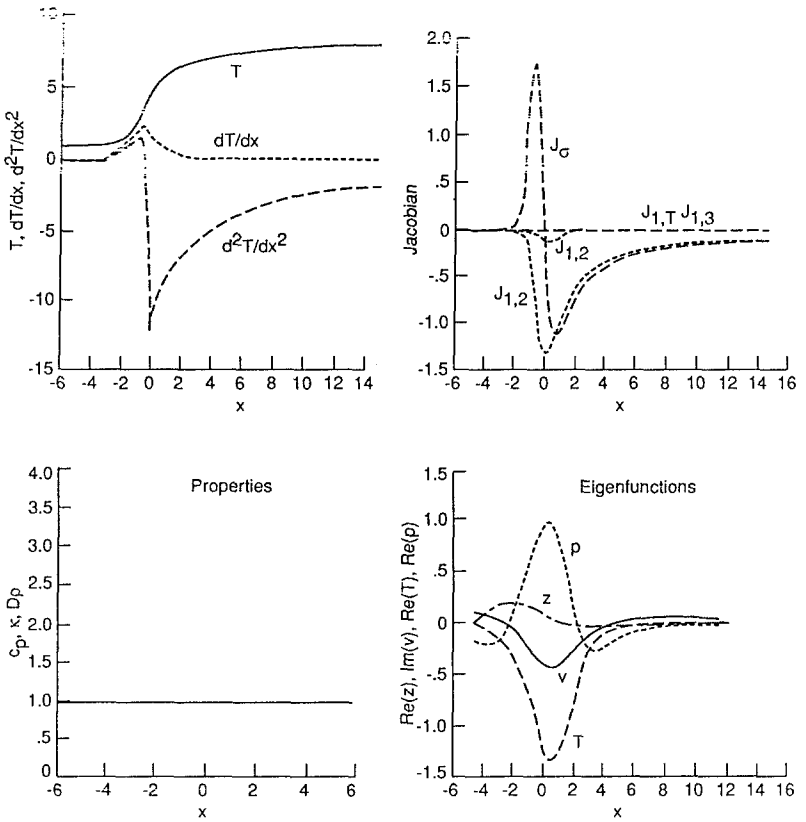

Fig. 6. Steady profiles, Jacobians, and eigenfunctions for $E = 16$ kcal/mole, $\delta_f = 0.06$ mm, $\mathrm{Le}_i = 1$, constant properties, and curve-fitted expressions.

wavelength to as large as 1.88 mm. The property variation that has caused the change is deduced from the next two results. Variable specific heat alone seems to slightly destabilise the flame. But conductivity and diffusivity variation coupled through the $Le = 1$ assumption is the most stabilising feature. It enhances the stability by a factor of three. Clavin [2] invoked the work of Clavin and Garcia [3] and has indicated that the variable property effects can be taken into account by the use of thermal diffusivity at the hot condition rather than the unburnt condition. This effectively amounts to taking δ_f about two to two and a half times higher than that estimated from the use of properties at unburnt condition. This effect then leads to enhanced stability. The results obtained in the current work are in conformity with the results of Clavin. The details can be understood by examining the results set out in Figs. 7 and 8. As can be noticed from these figures there are only weak differences in the profiles of the eigenfunctions, though the critical value of the wave number is significantly different between the constant and variable property case.

Results of the kind described for model reaction were again established in the present case. These are that (i) an increase of dT/dx by 1.5 changes the predicted

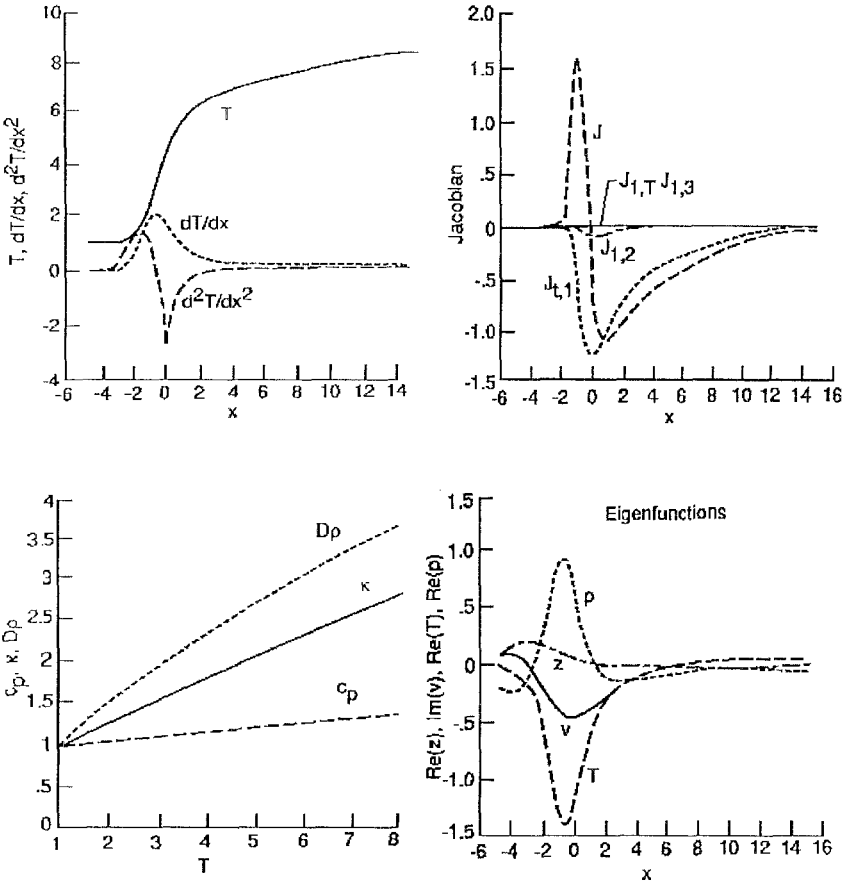

Fig. 7. Steady profiles, Jacobians, and eigenfunctions for $E = 16$ kcal/mole, $\delta_f = 0.06$ mm, $k = 0.20$, variable properties, and curve-fitted expressions.

critical wavelength by 2%, (ii) a change of (d^2T/dx^2) affects the results even less than a change in dT/dx, and (iii) an increase of the Jacobian profile by 10% causes increase of critical wave number of 25% (these results are not presented here).

Once the range of infinity (± 15) and the scheme for interpolation were established, the approach to curve fit the steady state quantities was abandoned in favor of numerically differentiating the temperature profile and using other interpolated quantities directly. Calculations for constant properties turned out to be straightforward and gave the results within 1% of those from the curve fit noted above. The calculations for variable properties turned out to be more difficult to perform and needed better resolution. This was accomplished with 151 grid points. (The CPU time for the calculations of the eigen spectrum and the eigen functions on Cray-2 super computer were 71 s for 121 grid points and 120 s for 151 grid points for one case).

Calculations have been made for two cases of nonunity Lewis number. In the first case, the Lewis number of all the species was 2. This corresponds to the conventional approach in which all Lewis numbers are equal. In the second case, the Lewis number

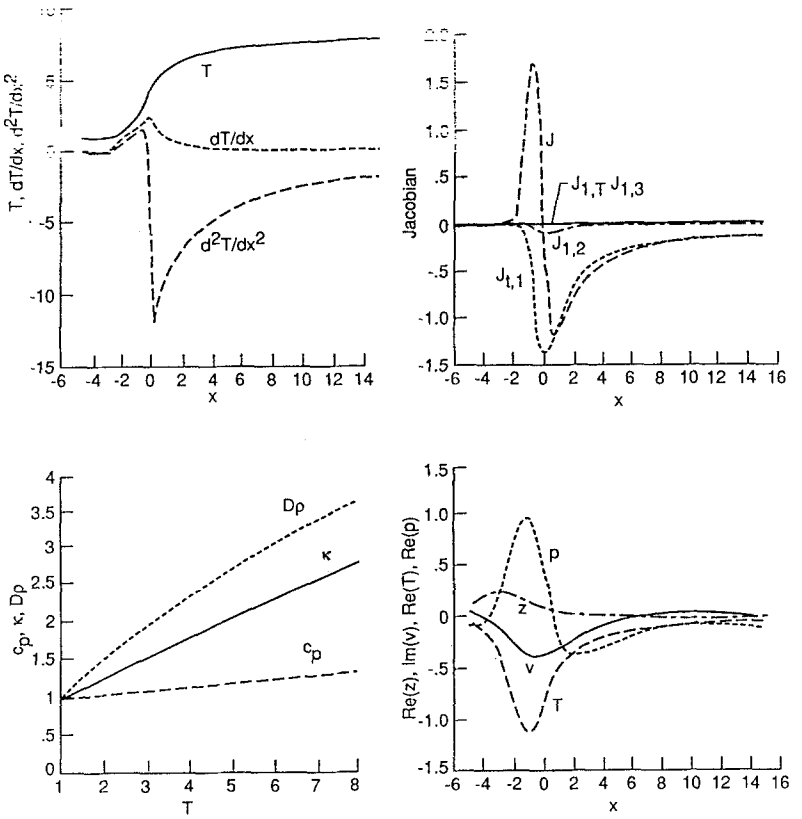

Fig. 8. Steady profiles, Jacobians, and eigenfunctions for $E = 16$ kcal/mole, $\delta_f = 0.06$ mm, constant properties, and derivatives numerically obtained.

of fuel alone is taken as 2.0 and the Lewis numbers of the other species were set to unity. This follows from the calculations of H_2-air either with full chemistry or single step chemistry with variable properties (see for instance, Bhashyam et al., [1]) which how that *Le* for H_2 is about 2–2.5, the *Le* for others is between 0.8 to 1.0. The steady state profiles of $Y_{i,s}$ versus T and the Jacobians are shown in Fig. 9. The profile shapes for $Le_i = 2$ show significant deviations from a linear profile. This is expected from simple analyses of the variation of nondimensional temperature with fuel mass fraction near a cold boundary [15]. The profiles for $Le_i = 2111$ (Lewis number of various species in order of H_2, O_2, H_2O, N_2), however, do not differ much from results with $Le = 1$. The difference in the results between $Le_i = 2111$ and $Le = 1$ are caused by the diffusion terms. The stability results are summarised in Table 4. The critical wavelength is typically 1.6–1.8 mm for the non-unity Lewis number cases. These values are only slightly smaller than the case $Le = 1$. These observed features are a consequence of the fact that hydrodynamics controls stability and details of flame structure are less relevent to stability.

Figure 10 shows the plots of the real and imaginary parts of the eigenvalues as a

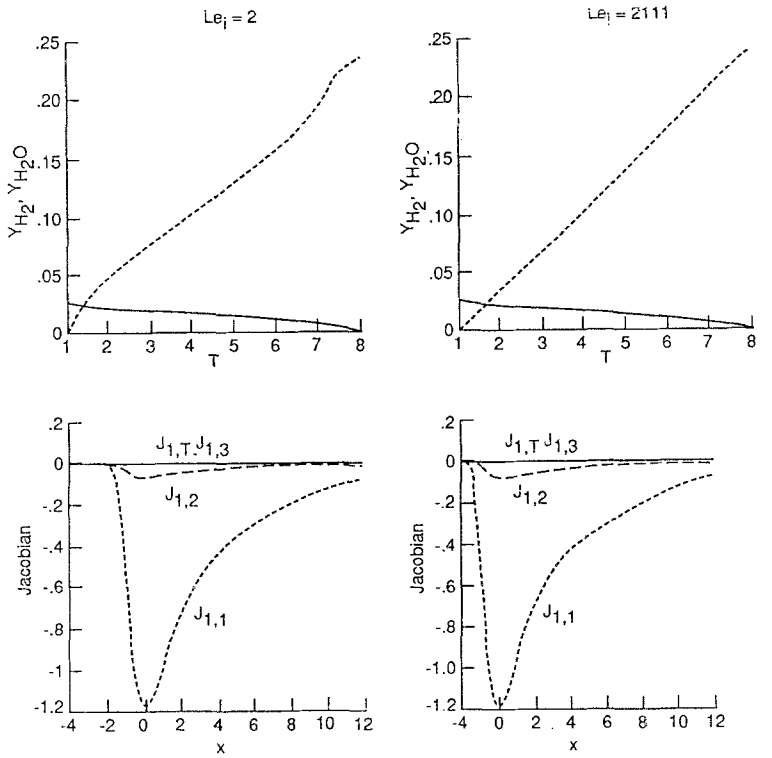

Fig. 9. Steady-state profiles of $Y_{i,s}$ and Jacobians for $Le_i = 2$ and 2111. $\delta_f = 0.06$ mm; $E = 16$ kcal/mole.

function of wave number, k. It may be noted that ω_r is less than 0 for the stable range shown by S in the figure. In all the cases excepting $Le_i = 2$ (with variable properties), the imaginary part (ω_i) is zero in the unstable range. The imaginary part being zero implies that the solution gets amplified in a non-oscillatory manner. The growth of the

Table 4. Case: Model B–continued

a. Critical wave number k_{crit} and δ_f

Case	k_{crit}	δ_f mm	*Wavelength*, mm $= 2\pi\delta_f/k_{crit}$
Const. prop., $Le_i = 2$	0.50	0.06	0.75
Var. prop., $Le_i = 2$	0.24	0.06	1.57
Const. prop., $Le_i = 2111$	0.48	0.06	0.785
Var. prop., $Le_i = 2111$	0.21	0.06	1.79

b. Peaks of eigen functions

Case	Rl z	Im v	Rl T	Rl p
Const. prop., $Le = 2$	9.5	23.0	86.4	60.4
Var. prop.	6.2	21.0	84.4	64.5

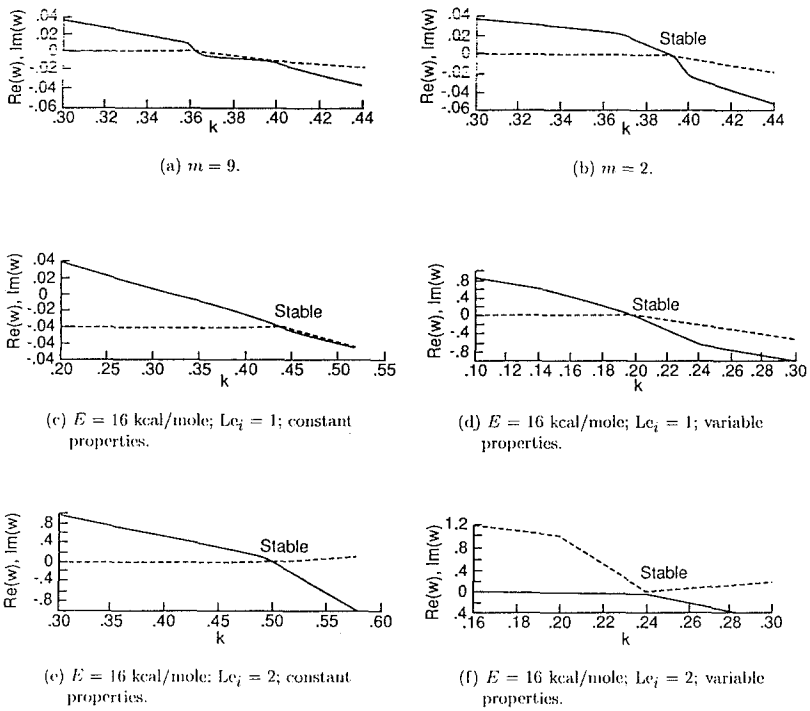

(a) $m = 9$.

(b) $m = 2$.

(c) $E = 16$ kcal/mole; $\mathrm{Le}_i = 1$; constant properties.

(d) $E = 16$ kcal/mole; $\mathrm{Le}_i = 1$; variable properties.

(e) $E = 16$ kcal/mole; $\mathrm{Le}_i = 2$; constant properties.

(f) $E = 16$ kcal/mole; $\mathrm{Le}_i = 2$; variable properties.

Fig. 10. Eigenvalues (real and imaginary) as function of wave number.

disturbance in time for any given unstable wavelength can be estimated from the results of Fig. 10. The time for doubling of disturbance amplitude can be obtained from the disturbance Eq. (16) as

$$t_{21,s} = \frac{0.693}{\omega_r(k)} \frac{\delta_f}{u_r}. \tag{50}$$

The time for doubling the amplitude scales like the characteristic time for the flame, the coefficient being typically about 5 to 20. These values will be relevent when making a full nonlinear simulation with a disturbance.

Concluding remarks

This paper has considered the problem of the stability of laminar flames, particularly the H_2-air system. The effects of finite rate kinetics and variable thermodynamic and transport properties are explored. The perturbation equations are spectrally discretized and numerically solved to obtain the eigenvalues and the corresponding eigenfunctions. These calculations show that

1. The effect of finite activation energy on the critical wavelength is not significant. Reduction of the activation energy to values corresponding to the H_2-air system reduces the critical wavelength by about 10%.
2. Variable transport properties enhance the stability and enhance the critical wavelength by a factor of 2–2.5.
3. Results for realistic parameters show that the critical unstable wavelength for stoichiometric the H_2-air mixture is about 1.8–1.9 mm.

Acknowledgements

These studies were performed while one of the authors (HSM) was a National Research Council Associate at NASA, LaRC. Thanks are due to Dr. Michel Macaraeg for help with her stability code and Dr. Balu Sekar and Dr. Craig Street for helpful discussions.

References

1. Bhashyam, A.T., Deshpande, S.M., Mukunda, H.S. and Goyal, G.: A novel operator splitting technique for one dimensional flame. *Comb. Sci and Tech.* 46 (1986) 223–248.
2. Clavin, P.: Dynamic behavior of premixed flame fronts in laminar and turbulent flows. *Prog. Energy Comb. Sci.* 11 (1985) 1–59.
3. Clavin, P. and Garcia, P.: The influence of the temperature dependence of diffusivities on the dynamics of flame fronts. *J. Mec. Therm. Appl.* 2 (1983) 245.
4. Darrieus, G., *Congress de Mecanique Appliquee* Paris (1945).
5. Fenn, J.B. and Calcote, H.F.: Activation energies in high temperature combustion, *Fourth Symposium (international) on Combustion* (1957) pp. 231–239.
6. Frankel, M.L. and Sivashinsky, G.I.: The effect of viscosity on the hydrodynamic stability of a plane flame front. *Comb. Sci. and Tech.* 39 (1982) 207–224.
7. Goyal, G., Paul, P.J., Mukunda, H.S. and Deshpande, S.M.: Further computational studies on the efficiency of operator split methods for one dimensional flames. *Comb. Sci. and Tech.* 43 (1989) 167–179.
8. Jackson, T.L. and Kapila, A.K.: Effect of thermal expansion on the stability of plane freely propagating flames. *Comb. Sci. and Tech.* 41 (1984) 191–201.
9. Jackson, T.L. and Kapila, A.K.: Effect of thermal expansion on the stability of plane freely propagating flames, Part II Incorporation of gravity and heat loss. *Comb. Sci. and Tech.* 49 (1986) 305–317.
10. Landau, L.: *Acta Physiochem, URSS* 19 (1944) 77.
11. Macaraeg, M.L., Street, C.L. and Hussaini, M.Y.: A spectral collocation solution to the compressible stability eigenvalue problem. *NASA TP* 2858 (1988).
12. Matalon, M. and Matkowsky, B.J.: Flames as gas dynamic discontinuities. *J. Fluid Mech.* 124 (1982) 239–259.
13. Mukunda, H.S., Deshpande, S.M. and Bhashyam, A.T.: New formulation for one dimensional premixed flames. *AIAA Jl* 24 (1986) 1127–1128.
14. Pelce, P., Clavin, P.: Influence of hydrodynamics and diffusion upon the stability limits of laminar premixed flames. *J. Fluid Mech.* 124 (1982) 219–237.
15. Spalding, D.B.: Predicting the laminar flame speeds in gases with temperature-explicit reaction rates, Parts I and II. *Comb. and Flame* 1 (1957) 287–307.